



BOND DENSITY AND PHYSICOCHEMICAL PROPERTIES OF A HYDROGENATED SILICON NITRIDE FILM

JOONG-WHAN LEE,^{†‡} RYONG RYOO,[†] MU SHIK JHON[†]
and KYOUNG-IK CHO[‡]

[†] Department of Chemistry and Center for Molecular Science, KAIST, Taeduk Science Town, Taejon, 305-701, Korea

[‡] Semiconductor Division, Electronics and Telecommunications Research Institute, P.O. Box 106, Yuseong, Taejon, 305-606, Korea

(Received 28 April 1994; accepted 3 June 1994)

Abstract—Hydrogenated silicon nitride films of 100–300 nm in thickness were prepared on GaAs and Si wafers by plasma enhanced chemical vapor deposition. The number of Si and N atoms in the film was measured by Rutherford backscattering. The number of H atoms was determined by an energy recoil detection (ERD) technique. A zero dose extrapolation method was employed to eliminate the effect of undesirable decrease in ERD count during ion-beam irradiation. The atomic density was determined by dividing the number of atoms by the film thickness obtained from ellipsometry. Infrared absorption cross sections of the Si—H and N—H bonds were obtained by using a correlation curve between IR band areas and the number of hydrogen atoms from ERD. The density of chemical bonds such as Si—Si, Si—N, Si—H and N—H was obtained by equating the atomic density with the absorption cross-section of the bonds. Investigation of the refractive index of films with different chemical structures suggests that a concept of the bond refraction can explain a relatively high refractive index (1.8–2.3) and low density ($2.1\text{--}2.7\text{ g/cm}^3$) of the Si-rich silicon nitride films, as compared with a stoichiometric compound Si_3N_4 . The etch rate of the silicon nitride film in buffered oxide etchant solution showed a linear relation against the density of silicon atoms that were not bonded to hydrogen.

Keywords: B. plasma deposition.

1. INTRODUCTION

Plasma enhanced chemical vapor deposited (PECVD) silicon nitride films receive great attention for applications in compound semiconductor technology because of their hardness, chemical inertness, and low-temperature adaptability [1]. However, wide variation of the film properties depending on details of the deposition process and conditions causes serious difficulties in controlling the film quality [2–5]. The PECVD silicon nitride films can be represented by a non-stoichiometric chemical formula, $\text{Si}_x\text{N}_y\text{H}_z$, with the atomic ratios depending considerably on the deposition process. The physical, electrical and optical properties of such hydrogenated silicon nitride films are known to depend on the Si/N atomic ratio and the hydrogen content [5–8].

The role of chemical bonds in the silicon nitride films appears to attract remarkable attention [4, 5, 9–12]. For example, the Si—Si bonds are suggested to be potentially harmful defects in a film for device applications [11], and the Si—H bonds enhance electrical properties of films by passivating Si dangling bonds [12]. It is clearly important to dis-

cover a good correlation between the macroscopic properties of the hydrogenated silicon nitride films and the local structure, i.e. the atomic bonding configuration.

In this work, we try to obtain very accurate information on the local bond density, such as [Si—H], [N—H], [Si—Si], and [Si—N] in a film by using Rutherford backscattering (RBS) and energy recoil detection (ERD) techniques and Fourier transform infrared spectroscopy (FTIR). The refractive index of the film and the etch rate in buffered oxide etchant (BOE) solution are our main interests concerning the local structure of the film. The films were prepared with a wide variety of deposition process parameters, such as flow rate of the reactant gas, chamber pressure, substrate temperature, ratio of the reactant gas, RF power, etc., in order to avoid prejudice that may come from limited deposition conditions.

2. EXPERIMENTAL DETAILS

Hydrogenated silicon nitride films were deposited on GaAs and Si wafers using a parallel plate of an RF

plasma system (IPL, 3000 PECVD) under the process conditions listed in Table 1. The set value in Table 1 represents a standard set of process parameters. Each sample was prepared by changing one of the set parameters into the variation as listed in Table 1.

The refractive index and thickness of the film on the GaAs wafer were measured with an ellipsometer (Rudolph, AutoEL-3). The wet etch rate of the film in 6:1 BOE solution (Baker, electronic grade) was measured at room temperature.

The $^4\text{He}^{++}$ backscattering spectra were obtained by using an RBS spectrometer (Charles Evans & Associates, RBS400) equipped with an ion accelerator (NEC, 3SDH). The He^{++} ion energy and ion beam charge were 2.5 MeV and 30 μC , respectively. The detector angle was 165° to the beam. The number of Si and N atoms per unit area was determined from the peak areas of the RBS spectrum. A silicon nitride film was deposited by low-pressure chemical vapor deposition (LPCVD). This film was used for calibrating the backscattering cross sections of the Si and N peak areas, with the assumption of a stoichiometric (Si_3N_4) compound. The atomic density was then obtained by dividing the number of atoms and bonds by the film thickness obtained from ellipsometry.

The ERD was performed with a glancing geometry [13] with the same equipment as the RBS. The ion dose was varied in the range 10–500 $\mu\text{C cm}^{-2}$ to observe the loss of the hydrogen counts induced by the ion beam. The sample surface and the detector were placed at angles of 15° and 30° to the beam, respectively.

The infrared (IR) absorption spectra were obtained using an FTIR spectrophotometer (Bomem, DA-8) with a mercury cadmium telluride detector in the range from 500 to 4000 cm^{-1} .

The Auger electron spectra were obtained by a VG microlab 310-D Auger electron spectroscopy (AES) after removing the surface contamination layer with 5 keV Ar^+ ion. The area ratios of Si-KLL/N-KLL and Si-LMM/N-KLL peaks were respectively measured and calibrated with those of an LPCVD Si_3N_4 film.

Table 1. Deposition conditions for the PECVD silicon nitride film

Process parameter	Set value	Variation
SiH_4/NH_3 flow ratio	0.4	0.2, 0.6
Pressure (Torr)	0.7	0.5, 1.0, 1.2
Temperature ($^\circ\text{C}$)	300	200, 400
RF Power (Watt)	30	15, 45
$\text{N}_2/(\text{SiH}_4 + \text{NH}_3)$ ratio	1	0, 2
$\text{SiH}_4 + \text{NH}_3$ flow rate (sccm)	50	20, 100

3. RESULTS AND DISCUSSION

3.1. Determination of atomic and bond density

The Si/N atomic ratio in the hydrogenated silicon nitride films was obtained by RBS and AES. Results from the two techniques show systematic disagreement in Fig. 1. The discrepancy may be attributed to the surface compositional changes that may occur due to ion-beam sputtering, which was applied before the AES analysis to remove contamination of the surface with the substitute oxide and carbon. This ion-beam sputtering can lead to the compositional change in the film surface. Moreover, the hydrogen-related bonds may break due to the primary electron beam in the AES analysis. In such cases, the peak sensitivity and the mean-free-path ratio of the Auger electron can change according to the compositional changes (i.e. matrix effect). Thus, the quantitative analysis of the hydrogenated silicon nitride with AES can include a significant error. A similar compositional change may also occur due to high-energy (MeV) ion beam for RBS. However, the decomposed elements other than hydrogen will remain in the film. It has been noted that the RBS technique is less sensitive to the surface change and has fewer matrix effects in principle [14]. It seems that the Si and N atomic densities (i.e. [Si] and [N]) measured by RBS are more accurate than that from an AES spectrum.

Accumulated ERD counts for the hydrogenated silicon nitride film are plotted in Fig. 2 against the dose of 2.5 MeV He^{++} ion beam. The films deposited at 200 and 300 $^\circ\text{C}$ show significant decreases in the ERD count with the ion beam dose. This result indicates that the hydrogen atom diffused out of the

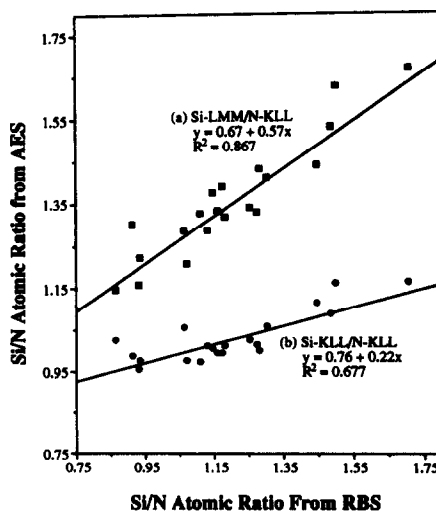


Fig. 1. Comparison between the Si/N atomic ratios obtained for the hydrogenated silicon nitride film by RBS and (a) Si—LMM/N—KLL, (b) Si—KLL/N—KLL peak area ratios in AES spectrum.

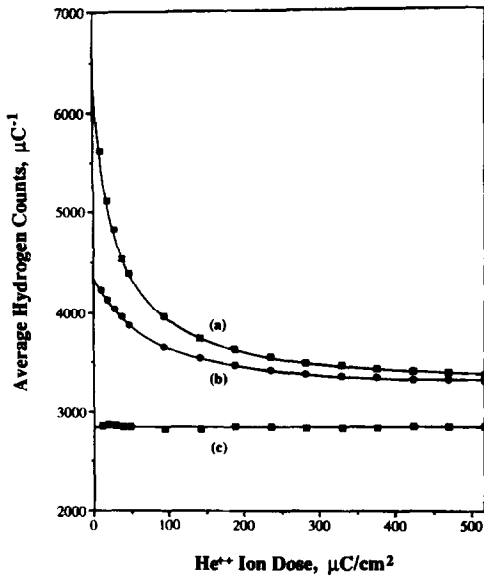


Fig. 2. Effect of 2.5 MeV He^{++} ion-beam irradiation on ERD hydrogen counts for the PECVD silicon nitride films deposited at (a) 200°C, (b) 300°C and (c) 400°C using a $\text{SiH}_4 + \text{NH}_3 + \text{N}_2$ gas mixture. The film thicknesses are (a) 2511, (b) 2118 and (c) 1740 Å, respectively.

film due to the ion beam irradiation damage. Such undesirable decreases in ERD counts can cause significant errors in the estimation of the H content. Therefore, the original ERD count at zero dose was obtained by an extrapolation of the measured ERD counts, as shown in Fig. 2. The number of hydrogen atoms in the film was determined by calibrating the original ERD counts extrapolated to zero dose with that of a polystyrene film (3410 Å thick) coated on an Si wafer.

It is worth noting that the PECVD silicon nitride film deposited at 400°C (Fig. 2(c)) shows no signifi-

cant changes in the ERD count. Thus, the hydrogen loss effect had a more dramatic influence on the films deposited at low substrate temperatures. Detailed results concerning the hydrogen loss during the ERD measurement will be reported separately [15].

IR absorption spectra of the films deposited on the GaAs wafer are shown in Fig. 3. The spectra were background-subtracted and normalized by the film thickness that was measured by ellipsometry. The absorption bands for asymmetric Si—N stretching (850 cm^{-1} , 1000 cm^{-1}), N—H deformation (1170 cm^{-1}), $\text{N}(\text{—H})_2$ deformation (1530 cm^{-1}), Si—H stretching (2160 cm^{-1}), N—H stretching (3350 cm^{-1}) and asymmetric $\text{N}(\text{—H})_2$ (3450 cm^{-1}) stretching vibration were observed. Deformation vibration of $\text{Si}(\text{—H})_2$ was expected to appear near 950 cm^{-1} . However, the presence of strong Si—H stretching vibration bands overlapping in the same region appears to make it difficult to distinguish the $\text{Si}(\text{—H})_2$ deformation.

The number of H atoms present in a hydrogenated silicon nitride film may be assumed equal to the total number of Si—H and N—H bonds, which can be obtained from the sum of the IR band areas (at 2160 and 3350 cm^{-1} , respectively) divided by the absorption cross sections. We estimated the IR band areas of a series of the PECVD films by multiplying the absorbance and the bandwidth at half-absorbance. We then adjusted the absorption cross sections until the number of H atoms obtained from the IR bands agreed best with that from the above ERD extrapolation method. The best fit was obtained with the absorption cross sections, $7.8 \times 10^{-18}\text{ cm}^2$ for Si—H and $5.1 \times 10^{-18}\text{ cm}^2$ for N—H, as shown in Fig. 4. Our results thus obtained agree remarkably with the cross sections, $7.4 \times 10^{-18}\text{ cm}^2$ for Si—H and

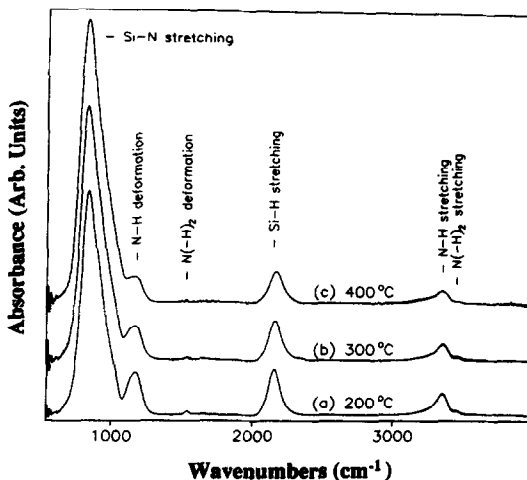


Fig. 3. IR absorbance spectra for the hydrogenated silicon nitride films deposited at (a) 200°C, (b) 300°C and (c) 400°C using a $\text{SiH}_4 + \text{NH}_3 + \text{N}_2$ gas mixture.

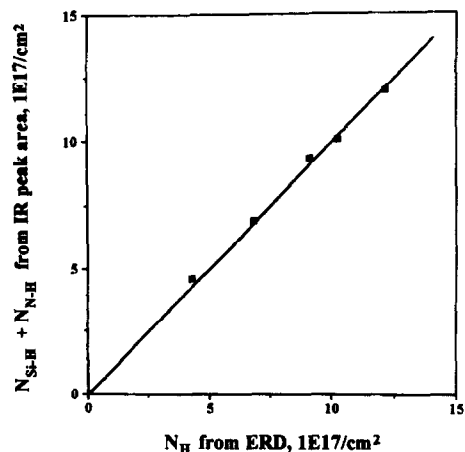


Fig. 4. Calibration curve for the total number of hydrogen related bonds ($N_{\text{Si-H}} + N_{\text{N-H}}$) from the IR peak areas versus the number of hydrogen atoms (N_{H}) obtained by ERD experiment.

$5.3 \times 10^{-18} \text{ cm}^2$ for N—H, which were determined by Lanford and Rand [16] using IR and a resonant nuclear reaction analysis (NRA) of PECVD silicon nitride films with thickness in the range 0.88–1.5 μm . The difference from our results with films 0.15–0.35 μm thick is less than 6%, as compared in Table 2. The IR band area can also be obtained by numerical integration using FTIR software. However, the band area by such numerical integration is somewhat greater because the IR absorption bands in Fig. 3 may not be represented by a simple statistical (i.e. Lorentzian or Gaussian) peak. If we use the integration method, the best-fitting cross sections are 9.4×10^{-18} and $6.0 \times 10^{-18} \text{ cm}^2$ for Si—H and N—H, respectively (Table 2).

The numbers of Si—H and N—H bonds listed in Table 1 were determined by multiplying the integrated band areas and the IR absorption cross sections. The bond densities, [Si—H] and [N—H], were then obtained by dividing the number of bonds by the film thickness. The following material balance eqns [5, 10] were employed in order to obtain the hydrogen atomic density, [H], and the bond densities, [Si—Si] and [Si—N]:

$$[\text{H}] = [\text{Si—H}] + [\text{N—H}] \quad (1)$$

$$3[\text{N}] = [\text{Si—N}] + [\text{N—H}] \quad (2)$$

$$4[\text{Si}] = 2[\text{Si—Si}] + [\text{Si—N}] + [\text{Si—H}] \quad (3)$$

Here, the values of Si and N atomic density were given from RBS. The N—N and H—H bonds were neglected because they were not likely to exist in the film in significant amounts. Moreover, the density of film (ρ) has the following relation with the values of atomic density:

$$\rho = \{[\text{Si}] \times 28.09 + [\text{N}] \times 14.01 + [\text{H}] \times 1.01\} / 6.023 \times 10^{23} \quad (4)$$

The results of solving eqns (1–4) are summarized in Table 3, for the samples prepared under 14 different deposition conditions. The refractive index and the etch rate of the films are also listed in Table 3.

3.2 Correlation between refractive index and bond density

The refractive index of the hydrogenated silicon nitride film is plotted in Fig. 5 against the Si/N atomic ratio obtained from RBS. Figure 5 does not show a good correlation between the refractive index and the Si/N ratio. This result appears to disagree with previous results that suggested strong positive correlations [6, 7, 10]. We observed that the refractive index increased with the Si/N atomic ratio when the ratio was changed by the variation of a single process parameter while all the other parameters were fixed. For example, the refractive index in Table 3 increased from 1.897 to 2.113 as the substrate temperature increased from 200 to 400°C. However, in this case the Si/N ratio remained nearly constant (1.075–1.080). The refractive index increased with the film density, but decreased against the hydrogen atomic density. It was thus difficult to find a general correlation between the refractive index and the Si/N atomic ratio.

In order to explain the refractive index of the silicon nitride film, we have adopted the concept of bond refraction that was originally introduced to explain the refractive index of organic compounds in terms of the molecular structure [17, 18]. According to the Lorentz–Lorentz equation, the molar refraction R_L is written by

$$R_L = (M/d)\{(n^2 - 1)/(n^2 + 2)\} \quad (5)$$

where M is the molecular weight, d is the density, and n is the refractive index. In a non-stoichiometric compound, such as the present hydrogenated silicon nitride, the molecular weight is not defined as a fixed

Table 2. Absorption cross sections for the Si—H and N—H infrared absorption band area of PECVD silicon nitride film

	Absorption cross section σ (cm^2)	
	Si—H (1965–2300 cm^{-1})	N—H (2950–3550 cm^{-1})
Area estimated by		
FWHM† \times absorbance		
—this work	7.8×10^{-18}	5.1×10^{-18}
—with NRA [16]	7.4×10^{-18}	5.3×10^{-18}
Computer aided integration‡		
—this work	9.4×10^{-18}	6.0×10^{-18}

† FWHM: full width at half maximum.

‡ Band area integrated using FTIR software.

Note: Number of H atoms per unit area can be obtained by $[\text{H}] = 1.06 \times 10^{17} \times \text{area}_{\text{Si—H}} + 1.68 \times 10^{17} \times \text{area}_{\text{N—H}} (\text{cm}^2)$.

Table 3. Bond and atomic densities for PECVD silicon nitride films obtained from FTIR and RBS analysis

Process parameter†	[Si]	[N]	[H]	[Si—Si]	[Si—N]	[Si—H]	[N—H]	Density (g cm ⁻³)	RI	Etch rate‡ (Å min ⁻¹)
	←			10 ²² /cm ³			→			
Set Value (see Table 1)	3.570	3.197	2.560	2.051	8.605	1.574	0.986	2.451	2.038	2346
SiH ₄ /NH ₃ = 0.2	3.245	3.525	2.666	1.104	9.340	1.431	1.235	2.378	1.855	8533
SiH ₄ /NH ₃ = 0.6	3.960	2.560	2.642	3.559	6.880	1.842	0.800	2.486	2.193	1352
SiH ₄ + NH ₃ = 20 sccm	3.360	3.635	2.510	1.392	9.526	1.131	1.379	2.454	1.880	2469
SiH ₄ + NH ₃ = 100 sccm	3.885	2.475	2.740	3.627	6.486	1.801	0.939	2.433	2.137	1959
Pressure = 0.5 Torr	3.520	2.930	2.390	2.512	7.728	1.328	1.062	2.363	2.006	1278
Pressure = 1.0 Torr	3.300	2.495	2.874	2.596	6.309	1.698	1.176	2.167	1.965	7922
Pressure = 1.2 Torr	3.500	2.880	2.858	2.220	7.671	1.889	0.969	2.350	1.968	10591
Temperature = 200°C	3.290	3.060	3.097	1.739	7.883	1.800	1.297	2.298	1.897	>20000
Temperature = 400°C	3.880	3.580	2.208	2.161	9.865	1.332	0.875	2.679	2.113	992
N ₂ /(SiH ₄ + NH ₃) = 0	3.608	2.690	2.890	2.275	8.157	1.726	1.164	2.454	2.017	4135
N ₂ /(SiH ₄ + NH ₃) = 2	3.370	2.870	2.331	2.200	7.679	1.400	0.931	2.278	1.986	2192
RF power = 15 Watt	3.950	3.058	2.641	2.926	8.180	1.767	0.874	2.588	2.097	1563
RF power = 45 Watt	3.430	2.811	2.484	2.494	7.341	1.392	1.092	2.295	2.004	2441

† Process parameters are the set values except for the indicated one.

‡ Etch rate in 6:1 buffered oxide etchant (NH₄/HF) at room temperature.

value. Thus, the molar refraction and the molar volume, $V_m = (M/d)$, are not appropriate to the non-stoichiometric compound. In that case, the refraction per unit volume ($= R_L/V_m$) can be used, and is related to the number of bonds in unit volume (i.e. bond density):

$$\begin{aligned}
 (n^2 - 1)/(n^2 + 2) &= R_L V_m \\
 &= R_{\text{Si-Si}} \frac{[\text{Si-Si}]}{N_A} + R_{\text{Si-N}} \frac{[\text{Si-N}]}{N_A} \\
 &+ R_{\text{Si-H}} \frac{[\text{Si-H}]}{N_A} + R_{\text{N-H}} \frac{[\text{N-H}]}{N_A} \quad (6)
 \end{aligned}$$

where N_A is Avogadro's number, and $R_{\text{Si-Si}}$, $R_{\text{Si-N}}$, $R_{\text{Si-H}}$ and $R_{\text{N-H}}$ are the molar refraction coefficients of Si—Si, Si—N, Si—H and N—H, respectively. Putting the values of refractive index and bond densities listed in Table 3 into eqn. (6) and adjusting the molar refraction coefficients, we obtained the best fit as shown in Fig. 6. The best fitting values of $R_{\text{Si-Si}}$, $R_{\text{Si-N}}$, $R_{\text{Si-H}}$ and $R_{\text{N-H}}$ are 4.51, 1.87, 2.12 and 1.31, respectively. It is remarkable that the molar refraction coefficients for Si—Si and Si—H are considerably higher than the others. Moreover, these bonds are not likely to exist in the stoichiometric Si₃N₄. The

contribution of these bonds seems to make the refractive index of the hydrogenated silicon nitride relatively high (1.8–2.3) as compared with 2.018 of Si₃N₄, in spite of its much lower density (2.1–2.7 g cm⁻³) than the 3.44 g cm⁻³ of Si₃N₄.

Figure 7 shows a simple correlation between the refractive index and the silicon atomic density of the film. This correlation is not as good as eqn (6). Nevertheless, a fairly good correlation can be

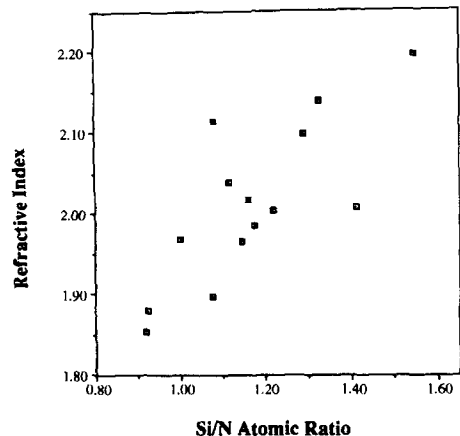


Fig. 5. Correlation between the Si/N atomic ratio measured by RBS and the refractive index of the hydrogenated silicon nitride film. The correlation coefficient $R^2 = 0.599$.

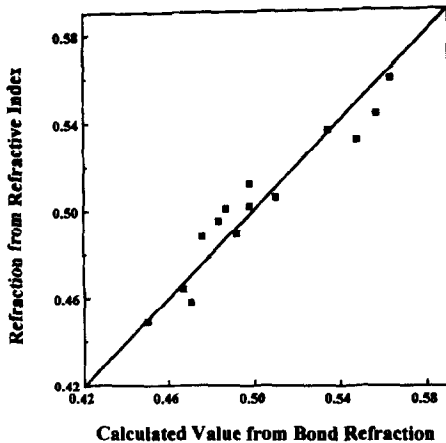


Fig. 6. Comparison between the experimental value of the refraction per unit volume and the theoretical value, $R_L/V_m = (n^2 - 1)/(n^2 + 2)$, calculated from bond concentrations of the film.

obtained because the Si—Si bond contributed most significantly to the refraction.

3.3 BOE etch rate and bond structure

Etch reaction of the hydrogenated silicon nitride films in a BOE solution consisting of NH_4F and HF (=6/1) may be considered to occur due to attack of the chemical bonds by the fluoride ion. Here, we assume the bond contributions to the etch rate in a manner analogous to the above bond refraction. Figure 8 shows a good linear relation between the logarithm of the etch rate and $[\text{Si—H}] + 0.39[\text{N—H}] - 0.53[\text{Si—Si}] - 0.17[\text{Si—N}]$. The positive coefficients for the Si—H and N—H bonds suggest that these “terminal” bonds are very susceptible to the etch reaction, while the negative

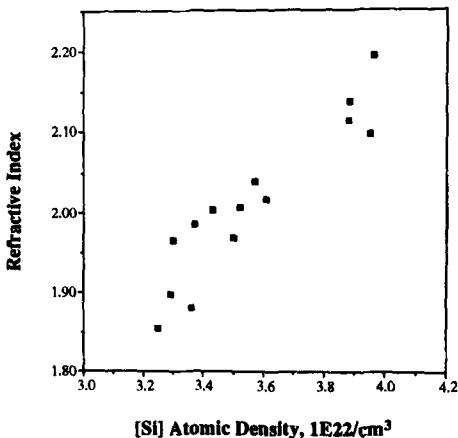


Fig. 7. Correlation between the refractive index and the silicon atomic density of the film. The correlation coefficient $R^2 = 0.864$.

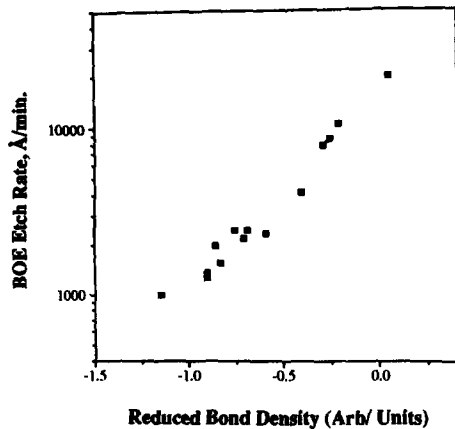


Fig. 8. Correlation between the etch rate of the film and a reduced bond density estimated from the bond contributions to the etch rate, i.e. $[\text{Si—H}] + 0.49[\text{N—H}] - 0.83[\text{Si—Si}] - 0.30[\text{Si—N}]$. The correlation coefficient $R^2 = 0.963$.

coefficients suggest that the Si—Si and Si—N “skeletal” bonds are more resistant. It is also worth noting that the coefficient for $[\text{Si—Si}]$ is lower than that of $[\text{Si—N}]$. Thus, the Si—Si bond in the hydrogenated silicon nitride film seems somewhat more resistant to the etch reaction than the Si—N bond.

The density of Si atoms in the PECVD silicon nitride films may be written as

$$[\text{Si}] = [=\text{Si}=\text{}] + [=\text{Si—H}] + [=\text{Si}(\text{—H})_2] + [—\text{Si}(\text{—H})_3] \quad (7)$$

where $=\text{Si}=\text{}$ represent silicon atom bonded to four Si or N atoms, $=\text{Si—H}$ refers to Si bonded to one H and three Si or N atoms, and so forth. Since the densities of $=\text{Si}(\text{—H})_2$ and $—\text{Si}(\text{—H})_3$ are very small

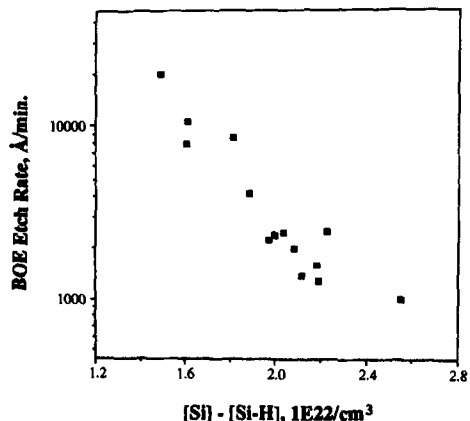


Fig. 9. Correlation between the etch rate of the film and the density of silicon atoms bonded to four Si or N atoms. The correlation coefficient $R^2 = 0.859$.

in the present hydrogenated silicon nitride film, $[≡Si-H] ≈ [Si-H]$ eqn (7) may be approximated to

$$[Si] ≈ [=Si=] + [≡Si-H]. \quad (8)$$

From eqn (8)

$$[≡Si=] ≈ [Si] - [≡Si-H]. \quad (9)$$

The $=Si=$ atom is the most highly cross-linked silicon atom, and therefore it is likely to be most highly resistant to the chemical etching. Figure 9 is shown to determine if there is a good correlation between the $[=Si=]$ and the etch resistance. Indeed, a good correlation can be found between the logarithm of the etch rate and $[Si] - [Si-H]$.

4. CONCLUSION

In order to determine the local bond density in the hydrogenated silicon nitride film, we have analysed the RBS, AES, ERD and FTIR spectra. Our results indicated that AES was not suitable for accurate analysis due to sample decomposition and matrix effects. The RBS data was very useful for the analysis of Si and N in the film. The ERD count had to be extrapolated to zero dose in order to take undesirable ion-beam irradiation effects into account for the H analysis. The IR absorption-band areas of Si-H (2160 cm^{-1}) and N-H (3350 cm^{-1}) bands agreed with this ERD analysis.

Our correlation between the film microstructure and refractive index or BOE etch rate can lead to the following conclusions. The refractive index can be well understood with the bond refraction. The refractive index has been shown to increase with the chemical bonds in the order $Si-Si > Si-H > Si-N > N-H$. The relatively high refractive index for the hydrogenated silicon nitride film with low density was obtained due to high density of Si-Si and Si-H bonds. The BOE etch rate can be ex-

plained with the bond densities. We have shown that the etch resistance decreases as $Si-Si > Si-N > N-H > Si-H$. Thus, high concentration of the Si-Si bonds can reduce the etch rate. However, it should be considered that the Si-Si bond is known to cause electrically harmful defects in device applications.

Acknowledgements—This work was partly supported by Ministry of Science and Technology, Korea.

REFERENCES

1. Valco G. J. and Kapoor V. J., *J. Electrochem. Soc.* **143**, 685 (1987).
2. Souk J. H., Parson G. N. and Batey J., *Mater. Res. Soc. Symp. Proc.* **219**, 787 (1991).
3. Shams Q. A. and Brown W. D., *Microelectron. J.* **20**, 49 (1989).
4. Khaliq M. A., Shams Q. A., Brown W. D. and Naseem H. A., *J. Electronic Mater.* **17**, 5 (1988).
5. Yin Z. and Smith F. W., *Phys. Rev.* **B42**, 3666 (1990).
6. Chang, M., Wong J. and Wang D. N. K., *Solid State Technol.* May, p. 193 (1988).
7. Fujita S., Toyoshima H., Ohishi T. and Sasaki A., *Jpn. J. Appl. Phys.* **23**, L144 (1984).
8. Kiermasz A. and Beekman K., *Semicond. Int.* June, p. 108 (1990).
9. Lee J. W., Cho K. I., Ryoo R. and Jhon M. S., *Proceedings of the State-of-the-Art Program on Compound Semiconductor XVIII*, p. 210, Electrochem. Soc. Inc, (1993).
10. Bustarret E., Bensouda M., Habrard M. C., Bruyere J. C., Poulin S. and Gujrathi S. C., *Phys Rev.* **B38**, 8171 (1988).
11. Jousse D. and Kanicki J., *Appl. Phys. Lett.* **55**, 1112 (1989).
12. Nguyen S. V., *J. Electronic Mater.* **16**, 275 (1987).
13. Lanford W. A., *Nuclear Instrum. Methods Phys. Res.* **B66**, 65 (1992).
14. Chu W. K., Mayer J. W. and Nicolet M. A., *Backscattering Spectrometry*, Academic Press, New York (1978).
15. Lee J. W., Lee S. H., Cho K. I., Jhon M. S. and Ryoo R., to be published.
16. Lanford W. A. and Rand M. J., *J. Appl. Phys.* **49**, 2473 (1978).
17. Batsanov S. S., *Refractometry and Chemical Structure*, Van Nostrand, New York (1966).
18. Vogel A. I., *Elementary Practical Organic Chemistry, 2nd Edition, Part 2, Qualitative Organic Analysis*, p. 24, Longman, New York (1966).